

# The Influence of Gradient Estimation on the Extraction of Boundary Point Cloud

Qian Huang, Thomas Wischgoll

Department of Computer Science, Wright State University  
Dayton, OH 43545

Email: {huang.11, thomas.wischgoll}@wright.edu

**Abstract**—To extract a tubular object boundary from a volumetric image is important to compute its morphometric properties, like the estimation of the boundary curvature, or the radius of a tubular object, for example, the radius is one of the descriptions of blood vessel for detecting the soft plaque. How to estimate the gradient of the volumetric data has an influence on the computation results of the morphometric properties. Extract the points of maximum gradient along the gradient direction in 3D as the boundary point cloud of an object is used by [4]. The boundary points are computed by trilinearly interpolated the volumetric datasets, and apply the parabolic interpolation to find the maximum gradient along the gradient direction. The extraction of boundary point cloud depends on the estimation of the image gradients. This paper is to compare the tricubic B-spline and trilinear interpolation algorithms on the estimations of morphometric properties of the volumetric dataset.

**Keywords**—gradient estimation, interpolation, boundary point cloud extraction, morphometric properties

## I. INTRODUCTION

The extraction of objects' boundaries are important in computer vision, image processing. A tubular object boundary can be used to estimate the boundaries' morphometric properties, boundary curvatures, or the radii of the tubular object. The image gradients are often used to define object boundaries, since object boundaries often generate sharp changes in image intensities. Extract the 3D points of maximum gradient along the gradient direction as the boundary points of an object is used by [4]. To extract a tubular object boundary from a volumetric image dataset is a sampling procedure from the discrete pixel/voxel grids. The boundary points are computed by interpolating the volumetric image dataset. Trilinear and tricubic B-spline (tensor product bezier form) are the two interpolation algorithms, which are compared in this paper.

## II. GRADIENT INTERPOLATION ALGORITHMS

### A. Trilinear Interpolation Algorithm

The trilinear interpolation assumes that the image intensity/gradient varies linearly between grid positions. A unit cube represents a voxel of a volumetric image dataset. Linearly interpolating points within such a cube is computed from the values of image intensities/gradients at each vertex, denoted as  $V_{000}$ ,  $V_{100}$ ,  $V_{010}$ , ...,  $V_{111}$ . The Paul Bourke interpolation equation is the following. The value of image intensities /gradients at position  $(x, y, z)$  is  $V_{xyz}$ .

$$\begin{aligned} V_{xyz} = & V_{000}(1-x)(1-y)(1-z) + V_{100}x(1-y)(1-z) \\ & + V_{010}(1-x)y(1-z) + V_{001}(1-x)(1-y)z \\ & + V_{101}x(1-y)z + V_{011}(1-x)yz \\ & + V_{110}xy(1-z) + V_{111}xyz. \end{aligned}$$

### B. Tensor Product Bezier Interpolation Algorithm

#### 1) Tensor product bezier intensity model

The tensor product bezier is built from curve, in which, the Bernstein polynomial is univariate function [1], [2]. This tricubic B-spline polynomial has 64 bezier points as the control net over the size of the voxel. The image intensity  $f(x, y, z)$  can be interpolated with such a tricubic subspace,  $b_{ijk}$  represents the bezier control point, in  $x, y, z$  directions. They are computed from the intensities and gradients at the grid positions among the volumetric image dataset. The image intensity inside a voxel is evaluated by the following interpolation equation

$$f(x, y, z) = \sum_{k=0}^3 \sum_{j=0}^3 \sum_{i=0}^3 b_{ijk} B_i^3(x) B_j^3(y) B_k^3(z)$$

$B_i^n(x) = \binom{n}{i}(1-x)^{n-i}x^i$  is the univariate Bernstein polynomial, here  $n = 3$ ,  $x \in [0,1]$ .

#### 2) Tensor Product Gradient Estimation

The image gradient is a directional change of the intensities in the image. They can be computed by differentiating this intensity model.

$$f_x = 3 \sum_{k=0}^3 \sum_{j=0}^3 \sum_{i=0}^2 (b_{i+1jk} - b_{ijk}) B_i^2(x) B_j^3(y) B_k^3(z)$$

$$f_y = 3 \sum_{k=0}^3 \sum_{j=0}^2 \sum_{i=0}^3 (b_{ij+1k} - b_{ijk}) B_i^3(x) B_j^2(y) B_k^3(z)$$

$$f_z = 3 \sum_{k=0}^2 \sum_{j=0}^3 \sum_{i=0}^3 (b_{ijk+1} - b_{ijk}) B_i^3(x) B_j^3(y) B_k^2(z)$$

$$b_{ijk} = f_{lmn} + a_0 * f_{lmn,x} + a_1 * f_{lmn,y} + a_2 * f_{lmn,z}$$

Inside a voxel, if  $i, j, k \in \{0,1\}$ , then  $l, m, n \in \{0\}$ ; and if  $i, j, k \in \{2,3\}$ , then  $l, m, n \in \{3\}$ . Also with  $i, j, k \in \{1\}$ ,

$\{a_0, a_1, a_2\} \in \{\frac{1}{3}\}$ ; with  $i, j, k \in \{2\}$ ,  $\{a_0, a_1, a_2\} \in \{-\frac{1}{3}\}$ ; and with  $i, j, k \in \{0, 3\}$ ,  $\{a_0, a_1, a_2\} \in \{0\}$ .

### 3) de Castejau Evaluation Scheme

To interpolate a gradient of a point  $(x, y, z)$  inside a voxel, the de Casteljau algorithm [1] is used to evaluate it. For example, the above gradient estimation equation can be rewritten as

$$f_x = 3 \sum_{k=0}^3 P_k(x, y) B_k^3(z), \text{ with}$$

$$P_k(x, y) = \sum_{j=0}^3 P_{jk}(x) B_j^3(y), \text{ and}$$

$$P_{jk}(x) = \sum_{i=0}^2 P_{ijk} B_i^2(x),$$

Here,  $(x, y, z) \in [0, 1] \times [0, 1] \times [0, 1]$ .

#### a) Evaluation of $P_{jk}(x)$

$$P_{ijk}^0 = P_{ijk} \text{ and } P_{ijk}^{p+1} = (1-x)P_{ijk}^p + xP_{i+1jk}^p$$

Then,  $P_{jk}(x) = P_{000}^2$ .

#### b) Evaluation of $P_k(x, y)$

$$P_{jk}^0(x) = P_{jk}(x) = P_{000}^2,$$

$$P_{jk}^{p+1}(x) = (1-y)P_{jk}^p(x) + yP_{j+1k}^p(x).$$

Then,  $P_k(x, y) = P_{000}^3(x, y)$ .

#### c) Evaluation of $f_x$

$$P_k^0(x, y) = P_k(x, y) = P_{000}^3$$

$$P_k^{p+1}(x, y) = (1-z)P_k^p(x, y) + zP_{k+1}^p(x, y)$$

Then,  $f_x = 3P_0^3(x, y, z)$ .

Through this gradient interpolation, the boundary point can be computed when the maximum gradient magnitude along gradient direction is found.

## III. THE MORPHOMETRIC PROPERTIES MEASUREMENT

This boundary cloud can build a surface with a triangle mesh. Let the boundary point has the normal at its associated grid position, thus the morphometric properties can be computed. The radius of the cylinder can be calculated when the boundary normal ray intersect the opposite the triangle mesh. The curvature of the boundary can also be obtained with its neighboring 1-ring triangles [3]. The means and deviations of the radius, curvature are analyzed.

The boundary point has an interpolated gradient estimated from trilinear or tensor product bezier interpolation algorithm. This interpolated gradient line has angles between its neighboring 1-ring triangles. These angles are averaged as the angle of this gradient line of its boundary point between its triangulated boundary surface.

Here two types of cylinder datasets are analyzed. They are of diameters of 10 pixels, 15 pixels respectively, pixel size is 0.24mm x 0.24mm. One image dataset has two parallel cylinders. The other has only one cylinder. Since all these boundary points of the cylinder have a uniform value of radius, maximum and minimum curvature, and angle of gradient line

between boundary surface. The mean and standard derivation of these values can be computed as criteria to the qualities of the extracted cylinders. All boundary points' radii construct a radius set, and the mean radius of these boundaries is the average of this radius set. The deviation is the standard deviation of these radius set. Similar methods are performed to maximum and minimum curvatures, also to the angles of gradient lines. All deviations' values shall be zeros. The theoretical mean value of maximum curvatures is the inverse of the radius of the cylinder, the theoretical mean value of the minimum curvatures are zeros. The mean angle of a gradient line between boundary surface shall be close to 90 degrees.

These two image datasets are smoothed with a recursive gaussian filter, the extracted boundary points are affected by the value of gaussian scale. The morphometric properties of the cylinders are measured under different gaussian scales.

## IV. ANALYSIS OF THE MEASUREMENT RESULTS

The extracted boundary point cloud can be visualized with a constraint delaunay triangle mesh. The angle of a gradient line with boundary surface can be computed from this triangle mesh. Also the radius of each boundary point, and curvature can be obtained.

### A. Triangulated Cylinders

Fig. 1 exhibits side and positive views of the triangulated one-cylinder extracted with the trilinear interpolation method, the gaussian scale is selected as 1mm. The short line associated with each boundary point is the interpolated gradient line. Fig. 2 displays two views of the extracted one-cylinder with trilinear method, the gaussian scale is 0.001mm. This cylinder is a little jagged compared with the cylinder extracted with 1mm of gaussian scale. Fig. 3 is the extracted one-cylinder with tensor product bezier interpolation algorithm, and their gaussian scale is 0.001mm. It is more jagged than the cylinder extracted with trilinear method in Fig. 2. Fig. 4 displays the one-cylinder obtained via tensor product bezier method, and the gaussian scale is 0.3mm. This cylinder has a coarser surface, then increase gaussian scale does not produce a smoother cylinder surface when tensor product bezier interpolation algorithm is applied. Fig. 5 and Fig. 6 illustrate the two-cylinders interpolated with trilinear and tensor product bezier methods, respectively, their gaussian scale is 0.2mm. Fig. 6 displays an unsmooth surface than that of Fig. 5. Fig. 7 represents the two-cylinder with trilinear interpolation method, and the gaussian scale is 0.8mm. And the shape of this two-cylinder deviates from the shape of a standard cylinder. When gaussian scale is 1.0mm, some boundary points between the two cylinders disappear, then the two cylinders extracted merge together when visualized with triangle mesh. It is shown in Fig. 8.

### B. Mean Angles and Derivations of Gradient Lines of Boundary Points between Boundary Surface

Fig. 9 displays the values of the angles of gradient line between the boundary surface at different gaussian scales. When the gradient line of the boundary is close to perpendicular to the triangulated cylinder surface, the mean angles will be near 90 degrees. The mean angles of one-cylinder with trilinear method approach 85 degrees when the

gaussian scale increases. The mean angles of two-cylinder with trilinear method will approach 85 degrees at gaussian scale=0.4mm, and start to decrease when gaussian scale increases.

And the mean angles of one-cylinder with tensor product bezier interpolation method are at much lower degrees, about 50 degrees. Also the gaussian scales increase, the mean angles have a trend of decreasing.

Fig. 10 exhibits the values of the derivations of the angles of the gradient lines between the boundary surfaces at different gaussian scales. If values of derivations approach to zero, the angles' values close to the mean. If the values of the derivations are large, it means the large differences among the values of the angles. The trend of the trilinear method is getting the lower derivation values than that of the tensor product bezier method.

The derivations of the angles with tensor product bezier method have rather higher values. These measurements indicate that the tensor product bezier interpolation method cannot get a smoother cylinder, when compared with trilinear interpolation method.

Since the angle of a gradient line between the surface of the standard cylinder should have a uniform value, close to 90 degree, the trilinear method extracts a more standard cylinder. For two-cylinder with trilinear method, when the gaussian scale increases, the recursive gaussian filter will convolve more neighboring voxels belonging to other object, so the shape of the extracted cylinders deviates those of the standard ones, and the mean angles and standard deviation values leave more from their uniform values.

Fig. 11 and Fig. 12 display the values of the mean angles and derivations with boundary points' gradients estimated from gradients at grid positions. For the tensor product bezier method, the mean angles are increased to above 65 degrees. Most of the derivations of the angles decrease much more also, and looks more perpendicular to the triangulated surface in Fig. 13. For trilinear method, the mean angles and derivations do not show obvious changes.

### C. Means and Derivations of Maximum Curvatures

Fig. 14 illustrates the mean values of maximum curvature at different gaussian scales. Fig. 15 shows the derivations of the maximum curvatures at different gaussian scales. The derivations of the maximum curvatures have a decreasing trend with the increment of gaussian scale, when trilinear interpolation method is applied. For one-cylinder dataset, at gaussian scale=1.0mm, the derivation of the maximum curvature decrease to  $0.001231 \text{ mm}^{-1}$ , the minimum value in the tested range. And the inverse of mean maximum curvature is 1.231mm, the one-cylinder has a radius  $5 \times 0.24 = 1.2\text{mm}$ , so the absolute error of radius estimated from maximum curvature is 0.03mm.

For two-cylinder dataset, at gaussian scale=0.4mm, the derivation of maximum curvature arrives the minimum value, and begin to increase when gaussian scale increases.

The one-cylinder, two-cylinder extracted by the tensor product bezier method have greater values of derivations of

maximum curvatures than those from trilinear method, which mean the extracted cylinders have unsmooth surfaces.

Fig. 16 exhibits the means of the minimum curvatures with varying gaussian scale's values, and Fig. 17 represents the derivations of the minimum curvatures. The zero values of the mean and derivations of minimum curvatures satisfy the standard cylinder properties. One-cylinder from trilinear method has zeros for the whole range of gaussian scales tested. For the two-cylinder, when gaussian scale is less than 0.6mm, the means and derivations of minimum curvatures can keep zero values. For the cylinder extracted from tensor product bezier method, when gaussian scale is greater than 0.1mm, the zeros of means and derivations of minimum curvatures are reached.

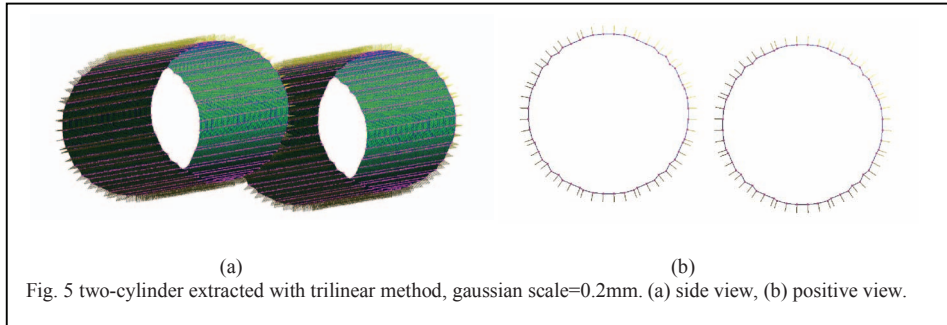
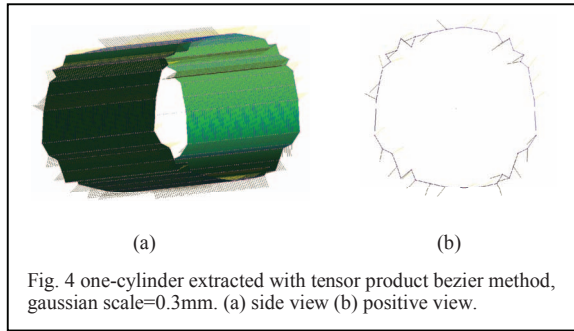
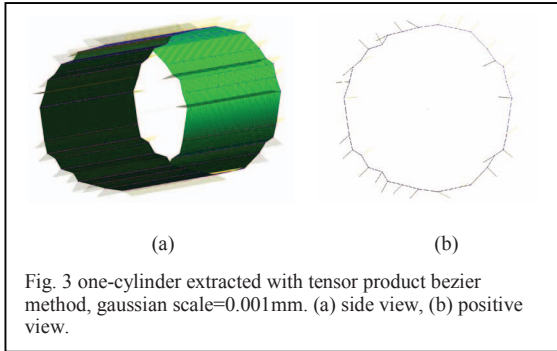
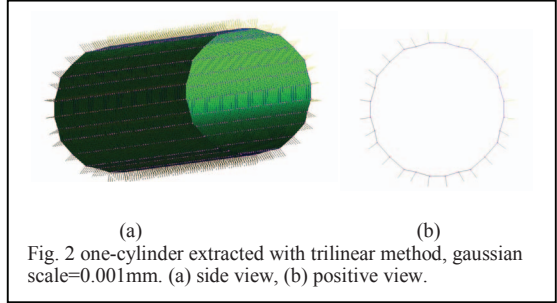
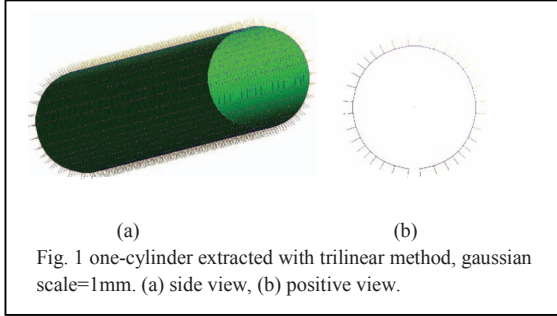
Fig. 18 and 19 display the means and derivations of the radii. Fig. 18 exhibits that the means of the radii computed from the trilinear and from tensor product bezier method have no significant difference. The radii of one-cylinder extracted from trilinear method change when the gaussian scale increases. At gaussian scale 1.0mm, the mean radius is 1.233mm, a difference of 0.002mm with the inverse of the maximum curvature. The derivations of the radii in Fig. 19 have lowest values for one-cylinder trilinear method, have lower values for two-cylinder from trilinear method at gaussian scales equaled to 0.2mm and 0.3mm. With the same gaussian scale condition, the derivations of radii from tensor product bezier method have a little high values than those from trilinear method for one-cylinder dataset.

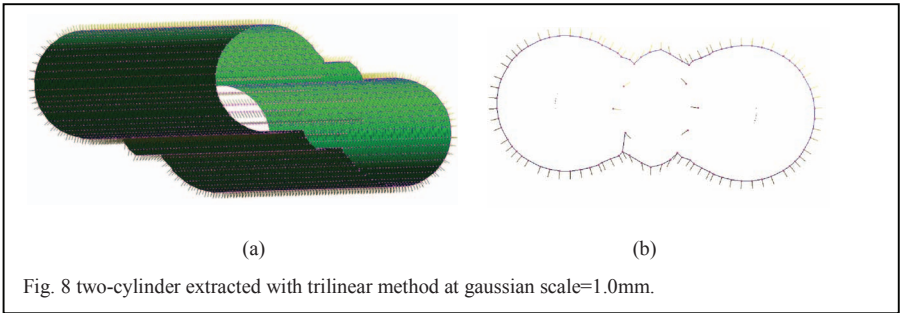
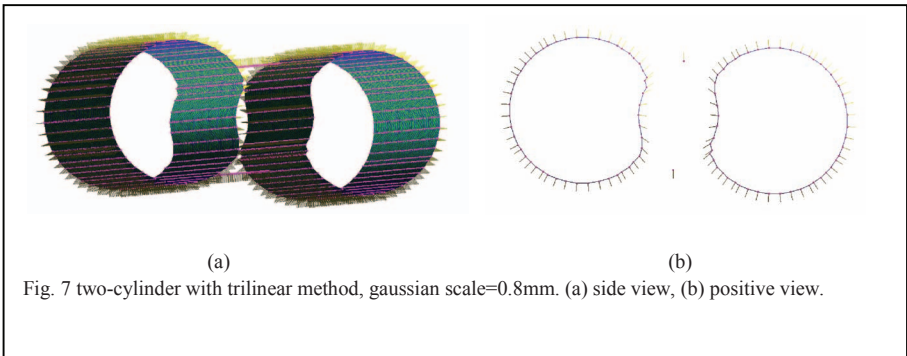
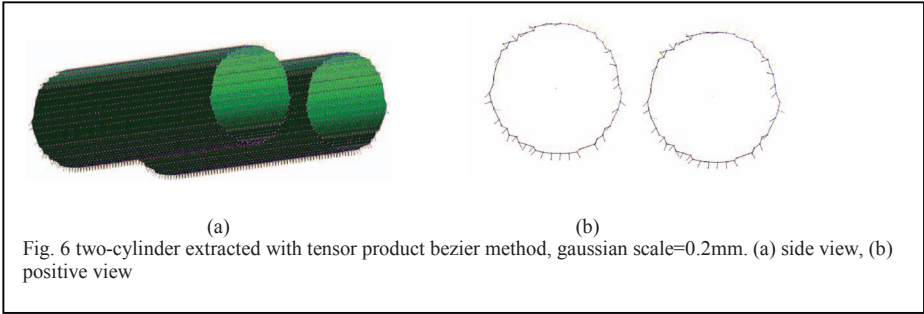
## V. CONCLUSION

The gradient estimated from trilinear interpolation method has different results on the extraction of boundary point cloud when compared with the tensor product interpolation method. The trilinear interpolation method exhibits more uniform values of angle of the gradient lines between the boundary surfaces, maximum and minimum curvatures, radius of the cylinder, these morphometric properties are owned by a standard cylinder. The relations of the recursive gaussian filter with different gaussian scales have been analyzed on the angles of the gradient lines, and the morphometric properties that have been measured. For trilinear method, it will produce a smoother boundary surface when the gaussian scale increase, and for tensor product bezier method, gaussian scale increment has no effect on obtaining a smoother boundary surface.

## REFERENCES

- [1] Gerald Farin, *Curves and Surfaces for Computer Aided Geometric Design, A Practical Guide*, Academic Press Inc., 1990.
- [2] Hartmut Prautzsch, Wolfgang Boehm, Marco Paluszny, *Bezier and B-spline techniques*, Springer 2002.
- [3] Gordon Kindlmann, Ross Whitaker, Tolga Tasdizen, Torsten Moller, *Curvature-Based Transfer Functions for Direct Volume Rendering: Methods and Applications*, Proceedings of the 14<sup>th</sup> IEEE Visualization 2003, pp. 513-520.
- [4] Thomas Wischgoll, Jenny Susana Choy, Erik L. Ritman, and Ghassan S. Kassab, *Validation of Image-Based Method for Extraction of Coronary Morphometry*, *annals of Biomedical Engineering*, Vol. 36, No. 3, March 2008 pp.356-368





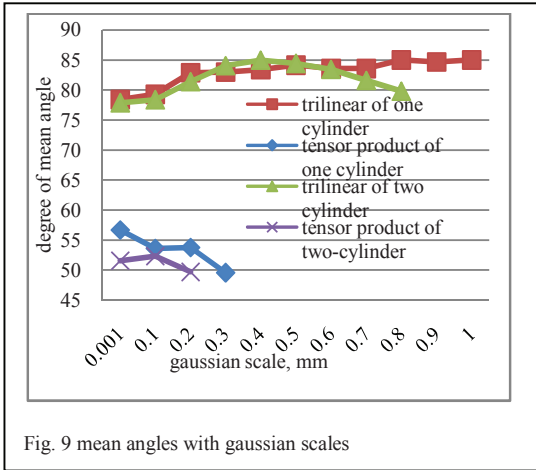


Fig. 9 mean angles with gaussian scales

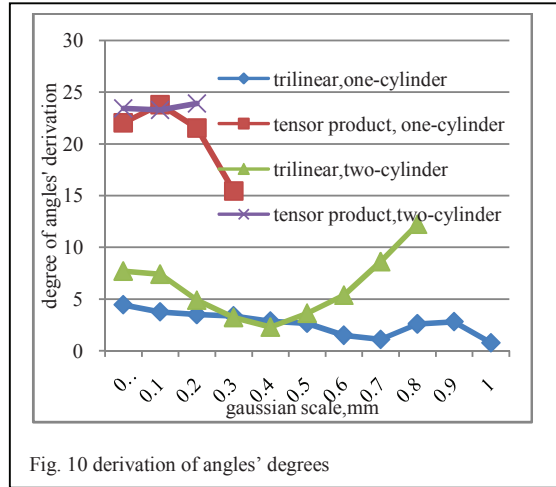


Fig. 10 derivation of angles' degrees

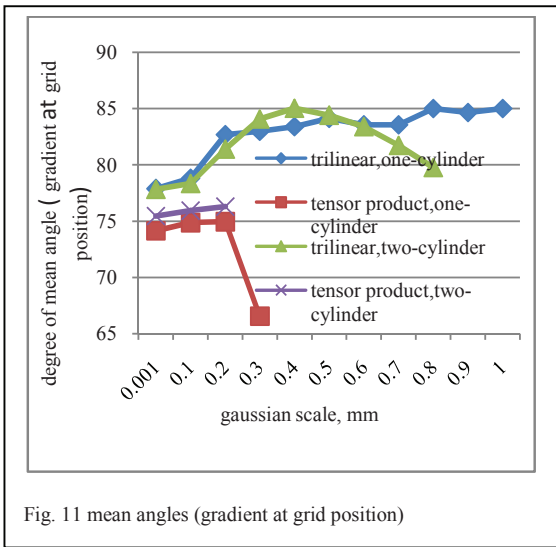


Fig. 11 mean angles (gradient at grid position)

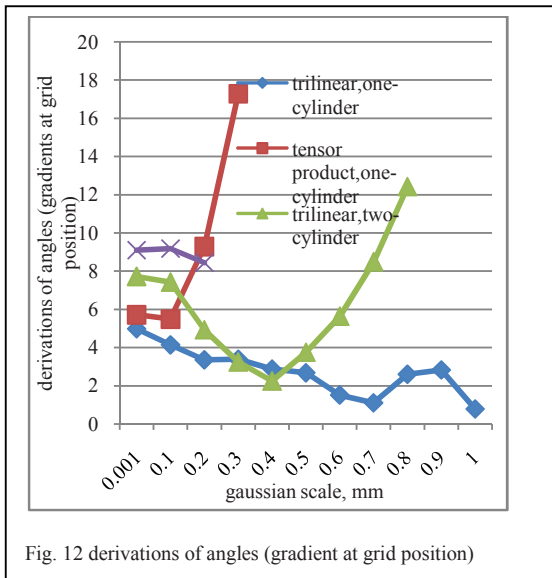
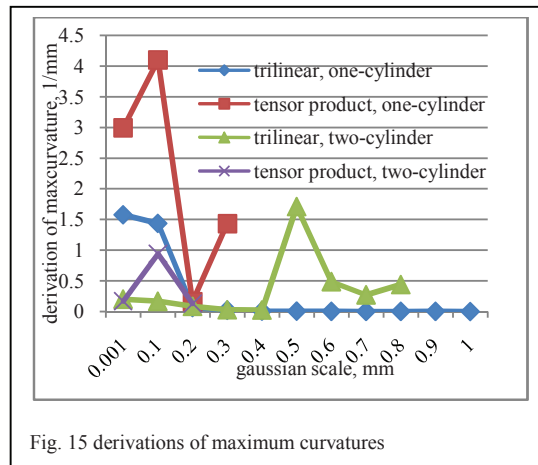
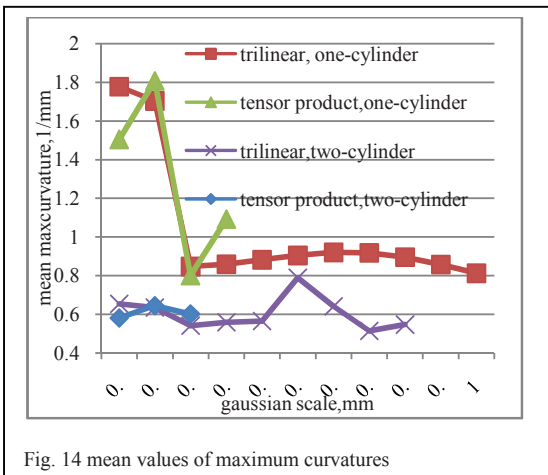
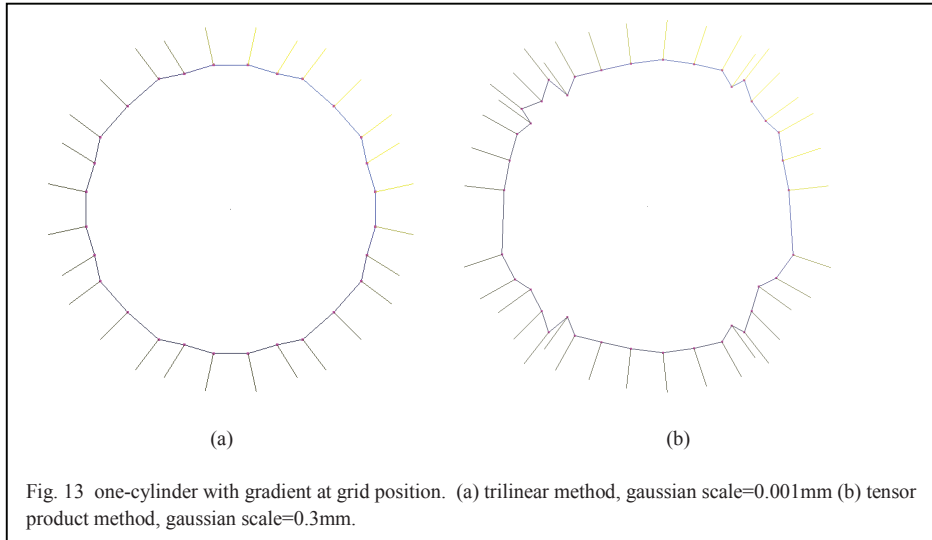


Fig. 12 derivations of angles (gradient at grid position)



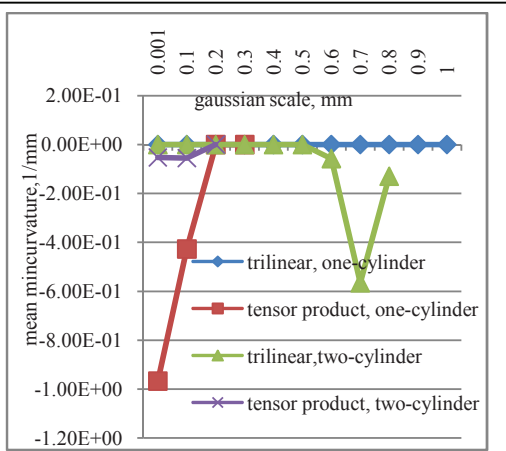


Fig. 16 mean of minimum curvatures

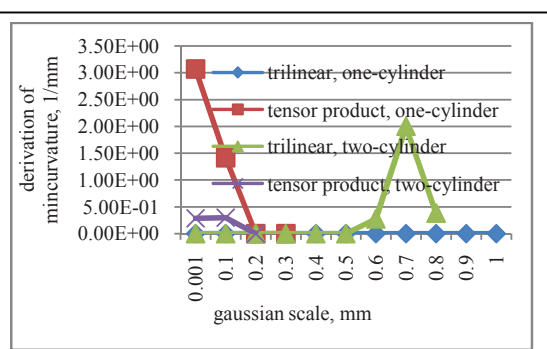


Fig. 17 derivations of minimum curvatures

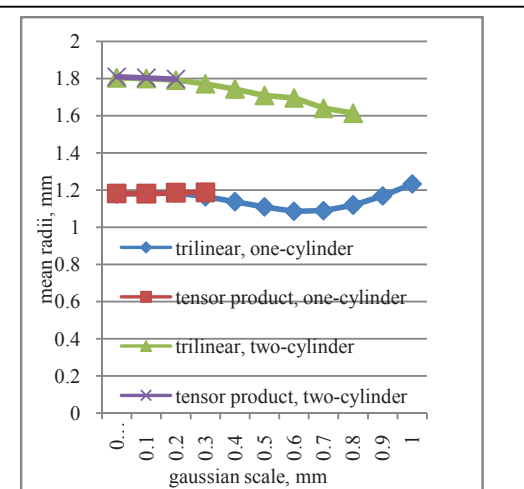


Fig. 18 mean of radii

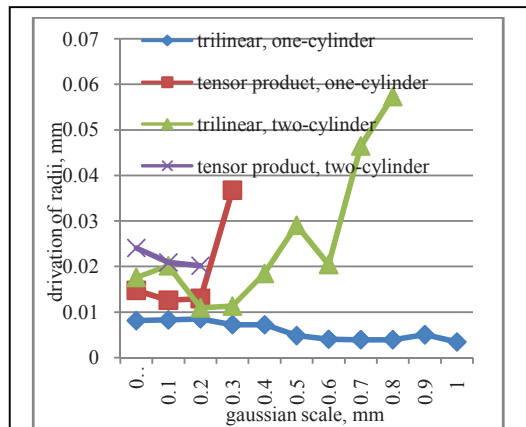


Fig. 19 derivation of radii